BEAM TRACKING FOR MOBILE MILLIMETER WAVE COMMUNICATION SYSTEMS

Vutha Va, Haris Vikalo, and Robert W. Heath Jr.
Wireless Networking and Communications Group, The University of Texas at Austin
Email: vutha.va@utexas.edu, hvikalo@ece.utexas.edu, rheath@utexas.edu

***Abstract*—Millimeter wave (mmWave) is an attractive option for high data rate applications. Enabling mmWave communications requires appropriate beamforming, which is conventionally realized by a lengthy beam training process. Such beam training will be a challenge for applying mmWave to mobile environments. As a solution, a beam tracking method requiring to train only one beam pair to track a path in the analog beamforming architecture is developed. Considering its low complexity which is suitable for mobile settings, the extended Kalman filter is chosen as the tracking filter. Several effects impacting the performance of the proposed tracking algorithm, such as the signal-to-noise ratio (SNR) and array size, are investigated. It is found that at the same SNR, narrower beams, which are more sensitive to angular changes, can provide more accurate estimate. Too narrow beams, however, degrade tracking performance because beam misalignment could happen during the measurement. Finally, a comparison to prior work is given where it is shown that our approach is more suitable for fast-changing environments thanks to the low measurement overhead.**

I. Introduction

Millimeter wave (mmWave) is a promising candidate for high data rate applications like wireless local area networks [1], [2], the fifth generation cellular (5G) networks [3], and vehicular networks [4]. Analog beamforming is often used in mmWave systems to provide transmit and receive beamforming gain. Accurate beamforming requires knowledge of the optimal pointing direction, which can be obtained through beam training at the expense of large overhead [5]–[7]. This is practical in static or slowly-changing environments but will become unacceptable for fast-changing environments, such as those in the vehicular context. Therefore, efficient beam training and tracking methods are important for enabling mmWave in mobile environments.

In this paper, we propose a beam tracking method suitable for mmWave communications in mobile environments under the analog beamforming architecture. One challenge of the analog architecture is the limited capability to perform measurement. With analog beamforming, only a fraction of the angular domain can be measured at a time. A full scan over all possible directions is a costly operation [6], [7], and thus should be avoided to the extent possible, especially in mobile environments. As a solution, we propose a beam tracking algorithm that uses only one measurement (i.e., not a full scan) when tracking a particular propagation path defined by a pair of Angle of Arrival (AoA) and Angle of Departure (AoD). This work uses a state-space approach to track the AoA and AoD of a given path. The extended Kalman filter (EKF) is chosen as the tracking filter. We investigate the effect of signal-to-noise ratio (SNR) and array size on the tracking capability. We find that larger arrays with narrower beams provide better tracking accuracy due to the higher sensitivity to changes in pointing directions. When the array becomes too large, however, the performance degrades because misalignment could happen during the measurement. Finally, a comparison to previous work [8] is provided. It is shown that due to the lower measurement overhead in our approach, it is more suitable for beam tracking in fast changing environments than the method in [8].

Prior work on beam tracking for mmWave systems includes [6], [8]–[10]. The beam tracking method proposed in [6] is based on detecting signal strengths via training sequences appended to data packets. This approach has been evaluated experimentally by monitoring adjacent beams (in the angular domain) in [9]. This approach requires to train multiple beam pairs, while our approach need to train only one beam pair. The work in [10] exploits the sparsity of the channel and reduces the problem of estimating the AoAs/AoDs to finding the support of the virtual channel matrix. Their tracking solution relies on the assumption that the previous estimate has small difference to the current AoA/AoD and does not exploit any dynamics of the channels. The most relevant prior work is that presented in [8], where a full scan of all possible beam combinations is used to create a measurement matrix to which EKF is applied. In contrast, our approach relies on a single measurement, i.e., at each step uses only one element of the measurement matrix in [8]. Also in our model, we allow time-variant path gains, while in [8] path gains are assumed fixed. A main drawback in [8] is the requirement for a full scan, which makes it difficult to track fast-changing environments due to the long measurement time. Our approach uses only a single measurement making it more suitable for tracking fast-changing channels.

II. System Model

This section describes the channel and its state-space model representation. We consider a time-varying geometric channel model which, at time k, is given by

$$\boldsymbol{G}[k] = \sum_{n=1}^{N[k]} \alpha_n[k]\boldsymbol{a}_{\mathrm{r}}(\phi_{n,\mathrm{A}}[k])\boldsymbol{a}_{\mathrm{t}}^{*}(\phi_{n,\mathrm{D}}[k]), \qquad (1)$$

where $(\cdot)^*$ denotes conjugate transpose, $N[k]$ is the number of paths, $\alpha_n[k]$ is the complex path gain, $\phi_{n,\mathrm{A}}[k]$ and $\phi_{n,\mathrm{D}}[k]$

are the AoA and AoD of the n-th path, respectively. $\boldsymbol{a}_{\mathrm{r}}(\cdot)$ and $\boldsymbol{a}_{\mathrm{t}}(\cdot)$ are the receive and transmit array response vectors, respectively. We assume uniform linear arrays (ULAs) at both the transmitter and the receiver. The array response vector of a ULA is given by

$$\boldsymbol{a}(\phi)=\frac{1}{\sqrt{M}}[1\ \ e^{\mathrm{j}\frac{2\pi}{\lambda}d\cos(\phi)}\ \ \ldots\ \ e^{\mathrm{j}(M-1)\frac{2\pi}{\lambda}d\cos(\phi)}]^{\mathrm{T}}, \quad (2)$$

with λ the carrier wavelength, d the antenna spacing, and M the number of antennas. For simplicity, here we restrict to 2D model so that we only need the angle in the azimuth. The extension of the tracking algorithm to 3D channel models using uniform planar arrays is straightforward.

Next, we describe the measurement model. Recall that we are interested in tracking a single propagation path so that transmit and receive beams can be adjusted accordingly to maintain the alignment. Multiple paths can be tracked separately by using the method to be described in Section III in parallel. The received signal when using a beamformer $\boldsymbol{f}$ and a combiner $\boldsymbol{w}$ can be written as

$$\begin{aligned} y[k]&=\alpha_i[k]\boldsymbol{w}^*\boldsymbol{a}_{\mathrm{r}}(\phi_{i,\mathrm{A}}[k])\boldsymbol{a}_{\mathrm{t}}^*(\phi_{i,\mathrm{D}}[k])\boldsymbol{f}\\ &\quad+\sum_{n\neq i}\alpha_n[k]\boldsymbol{w}^*\boldsymbol{a}_{\mathrm{r}}(\phi_{n,\mathrm{A}}[k])\boldsymbol{a}_{\mathrm{t}}^*(\phi_{n,\mathrm{D}}[k])\boldsymbol{f}+\nu[k] \quad (3)\\ &=\alpha_i[k]\boldsymbol{w}^*\boldsymbol{a}_{\mathrm{r}}(\phi_{i,\mathrm{A}}[k])\boldsymbol{a}_{\mathrm{t}}^*(\phi_{i,\mathrm{D}}[k])\boldsymbol{f}+v[k]. \quad (4)\end{aligned}$$

The mmWave channel is commonly assumed to be sparse [11], [12]. Here, it is assumed that the sparsity makes the paths to be likely separated from each other, and only a single path falls into the main beam direction (this assumption is more accurate as the beam becomes narrower). All other paths fall into the sidelobe directions and will be treated as noise aggregated in the noise variable $v[k]$ in (4).

We now describe the state evolution model. We define the state vector by

$$\boldsymbol{x}[k]=\left[\alpha_{\mathrm{R}}[k],\alpha_{\mathrm{I}}[k],\phi_{\mathrm{A}}[k],\phi_{\mathrm{D}}[k]\right]^{\mathrm{T}}, \quad (5)$$

where $\alpha[k]=\alpha_{\mathrm{R}}[k]+\mathrm{j}\alpha_{\mathrm{I}}[k]$ and we drop the path index i as we concern only with the tracking of this path. Note that by using the real and imaginary part of $\alpha[k]$, the state vector $\boldsymbol{x}[k]$ is a real vector which helps avoid implementation issues when real and complex numbers are mixed. We assume $\alpha_i[k]$ follows the first-order Gauss-Markov model given by

$$\alpha_i[k+1]=\rho\alpha_i[k]+\zeta[k], \quad (6)$$

where ρ is the correlation coefficient, $\zeta[k]\sim\mathcal{N}(0,(1-\rho^2)/2)$, $i\in\{\mathrm{R},\mathrm{I}\}$, and $\alpha_i[-1]\sim\mathcal{N}(0,1/2)$. We assume a generic evolution model for the AoA/AoD that is driven by a Gaussian process noise. The state evolution can now be written as

$$\boldsymbol{x}[k]=\boldsymbol{F}\boldsymbol{x}[k-1]+\boldsymbol{u}[k-1], \quad (7)$$

where $\boldsymbol{F}=\mathrm{diag}([\rho,\rho,1,1])$ with $\mathrm{diag}(\boldsymbol{a})$ denoting the diagonal matrix whose diagonal elements form the vector $\boldsymbol{a}$. It is assumed that the AoA and AoD are independent of each other and $\alpha[k]$ so that $\boldsymbol{u}[k]\sim\mathcal{NC}(\boldsymbol{0},\boldsymbol{\Sigma}_{\boldsymbol{u}})$ with

$$\boldsymbol{\Sigma}_{\boldsymbol{u}}=\mathrm{diag}(\left[1-\rho^2,1-\rho^2,\sigma_{\mathrm{A}}^2,\sigma_{\mathrm{D}}^2\right]). \quad (8)$$

To complete our state-space model, we need to derive the measurement function. A common method to steer a ULA driven by phase-shifters at a direction $\bar{\phi}$ is the approach using progressive phase-shift [13]. With this method, the feed coefficients to each element of the ULA can be written as $[1\ e^{\mathrm{j}\frac{2\pi}{\lambda}d\cos(\bar{\phi})}\ \ldots\ e^{\mathrm{j}(M-1)\frac{2\pi}{\lambda}d\cos(\bar{\phi})}]^{\mathrm{T}}/\sqrt{M}=\boldsymbol{a}(\bar{\phi})$. Note that all the feed coefficients have the same amplitude. This is the constant amplitude constraint of the phase-shifters. (If amplitudes can be varied, more sophisticated methods rather than progressive phase shift can be used that have better control over the beamwidth and sidelobe [13].) Let $\bar{\phi}_{\mathrm{A}}$ be the pointing direction of the combiner $\boldsymbol{w}$, we have

$$\boldsymbol{w}^*(\bar{\phi}_{\mathrm{A}})\boldsymbol{a}_{\mathrm{r}}(\phi_{\mathrm{A}})=\frac{1}{N_{\mathrm{r}}}\frac{1-e^{\mathrm{j}N_{\mathrm{r}}kd(\cos\phi_{\mathrm{A}}-\cos\bar{\phi}_{\mathrm{A}})}}{1-e^{\mathrm{j}kd(\cos\phi_{\mathrm{A}}-\cos\bar{\phi}_{\mathrm{A}})}} \quad (9)$$

where we have used the formula $\sum_{i=0}^{M-1}a^i=(1-a^M)/(1-a)$. Similarly, let $\bar{\phi}_{\mathrm{D}}$ be the pointing direction of the beamformer $\boldsymbol{f}$, we can compute $\boldsymbol{a}_{\mathrm{t}}^*(\phi_{\mathrm{D}})\boldsymbol{f}(\bar{\phi}_{\mathrm{D}})$. Define $\Phi_{\mathrm{A}}=\cos\phi_{\mathrm{A}}-\cos\bar{\phi}_{\mathrm{A}}$ and $\Phi_{\mathrm{D}}=\cos\phi_{\mathrm{D}}-\cos\bar{\phi}_{\mathrm{D}}$, the received signal can be written as

$$y[k]=\underbrace{\frac{\alpha[k]}{N_{\mathrm{r}}N_{\mathrm{t}}}\frac{1-e^{\mathrm{j}N_{\mathrm{r}}kd\Phi_{\mathrm{A}}}}{1-e^{\mathrm{j}kd\Phi_{\mathrm{A}}}}\frac{1-e^{\mathrm{j}N_{\mathrm{t}}kd\Phi_{\mathrm{D}}}}{1-e^{\mathrm{j}kd\Phi_{\mathrm{D}}}}}_{h(\boldsymbol{x}[k];\bar{\phi})}+v[k], \quad (10)$$

where N_{r} and N_{t} are the number of receive and transmit antennas, respectively.

III. Beam Tracking Algorithm

An overview of the proposed beam tracking is illustrated in Fig. 1. It is assumed that there is an AoA/AoD estimator that could output estimates to be used as the starting point for the tracking algorithm. The beam tracking algorithm starts with setting a pair of transmit and receive beams according to the estimated AoA and AoD from the AoA/AoD estimator. Note that $\bar{\phi}$ is the pointing direction of the beam and is a parameter in the measurement function $h(\cdot;\bar{\phi})$ defined in (10). It is desired that the difference between $\bar{\phi}$ and $\hat{\phi}$ be small so that the beams stay aligned (i.e., within half the beamwidth). If this cannot be kept, $h(\boldsymbol{x};\bar{\phi})$ will become small and the SNR of the observation $y[k]$ degrades and the tracking divergence will accelerate. Since the tracking error accumulates with time, the validity should be checked against some threshold ϕ_{th}. The path itself could also disappear at some point in time (e.g., due to blockage). If it is detected that the tracking is no longer reliable or the path does not exist anymore, the AoA/AoD should be re-estimated. This work focuses on the tracking part and leaves the shaded blocks for future work.

For the choice of tracking algorithms, we choose the EKF. The EKF is a popular choice for nonlinear problems due to its low complexity and good performance if the nonlinearity is "mild" [14].

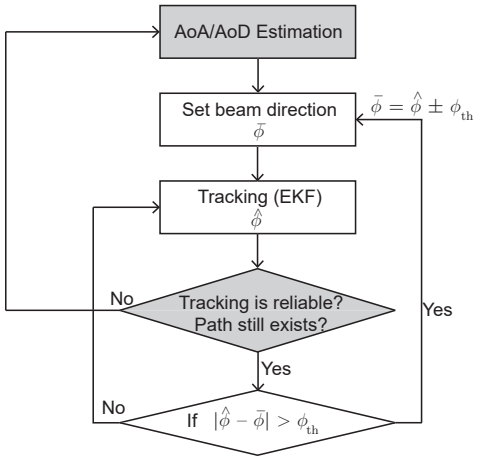

Fig. 1. An overview of the proposed tracking algorithm. The two shaded blocks are not considered in this work. They are necessary to complete this system and will be considered in future work.

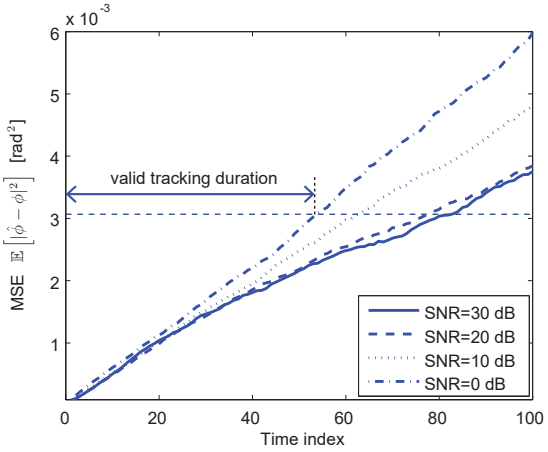

Fig. 2. This figure shows the MSE of the AoA defined by $\mathbb{E}\left[|\phi[k] - \hat{\phi}[k]|^2\right]$ for each time instance at different SNRs. The dashed straight line shows the MSE corresponding to the error of one half beamwidth.

The EKF recursion is given in the following [15].

$$\hat{\boldsymbol{x}}[k|k-1] = \hat{\boldsymbol{x}}[k-1|k-1] \tag{11}$$

$$\boldsymbol{K}_{f,k} = \boldsymbol{P}_{k|k-1}\boldsymbol{H}_k^* \frac{1}{\boldsymbol{H}_k \boldsymbol{P}_{k|k-1}\boldsymbol{H}_k^* + \sigma_v^2} \tag{12}$$

$$\hat{\boldsymbol{x}}[k|k] = \hat{\boldsymbol{x}}[k|k-1] + \boldsymbol{K}_{f,k}\left\{y[k] - h(\hat{\boldsymbol{x}}[k|k-1])\right\} \tag{13}$$

$$\boldsymbol{P}_{k|k} = (\boldsymbol{I} - \boldsymbol{K}_{f,k}\boldsymbol{H}_k)\boldsymbol{P}_{k|k-1} \tag{14}$$

$$\boldsymbol{P}_{k+1|k} = \boldsymbol{P}_{k|k} + \boldsymbol{\Sigma}_{\boldsymbol{u}}, \tag{15}$$

where $\boldsymbol{H}_k = \nabla_{\boldsymbol{x}} h|_{\boldsymbol{x}=\hat{\boldsymbol{x}}[k|k-1]}$ which is the gradient of the measurement function. By assumption of the model $\boldsymbol{Q}_k = \boldsymbol{\Sigma}_{\boldsymbol{u}}$ does not change with time. The initialization conditions are

$$\hat{\boldsymbol{x}}[0|-1] = \hat{\boldsymbol{x}}_0, \tag{16}$$

$$\boldsymbol{P}_{0|-1} = \boldsymbol{\Sigma}_{\boldsymbol{u}}, \tag{17}$$

where $\hat{\boldsymbol{x}}_0$ is the estimate from the AoA/AoD estimator. The rational for the choice of $\boldsymbol{P}_{0|-1}$ is that if we have an accurate AoA/AoD estimator that performed the estimation one time slot prior to the tracking, the error will be mainly due to the dynamics of the system which is determined by the process noise $\boldsymbol{u}$. Note that in the implementation, we redefine $\tilde{\boldsymbol{y}}[k] = [\Re(y[k]), \Im(y[k])]^{\mathrm{T}}$, $\tilde{\boldsymbol{H}}[k] = [\Re(H[k]), \Im(H[k])]^{\mathrm{T}}$, so that we only deal with real numbers.

IV. Numerical Results and Discussion

In this section, we numerically investigate the performance of the tracking algorithms. We study the effect of SNR, array size, and provide a comparison to prior work in [8].

A. Effect of SNR

Fig. 2 shows the mean square error (MSE) performance of the tracking algorithm at different SNRs. Here we only show the AoA because the AoD behaves similarly and $\alpha[k]$ is not of concern in the alignment process. The SNR here includes the antenna gain. In this simulation, $N_{\mathrm{t}} = N_{\mathrm{r}} = 16$, the initial AoA and AoD of $45°$, $\rho = 0.995$, and $\sigma_{\mathrm{A}}^2 = \sigma_{\mathrm{D}}^2 = (0.5°)^2$ are used. Note that although $0.5°$ angular variation seems very small, one should note that the duration of a time slot here can be on the millisecond order or less (duration of one data packet) and this actually corresponds to rather fast angular changes. Each MSE plot is obtained by averaging over 5000 simulation runs.

TABLE I
Valid tracking duration in number of time slots.

SNR [dB]	−10	0	10	20	30
AoA	45	53	62	77	82
AoD	44	52	64	74	78

Fig. 2 shows the MSE of the tracking algorithm against time index for SNR of 0, 10, 20, and 30 dB. We see that the difference between 30 dB and 20 dB is small, while the differences at lower SNRs are much more noticeable.

To provide a sense of how long the tracking stays valid, we determine the time index where the MSE exceeds a given threshold. An illustration of the valid tracking duration for SNR of 0 dB is shown in Fig. 2. The choice of the threshold used here is $\sqrt{\mathbb{E}\left[|\phi[k] - \hat{\phi}[k]|^2\right]} = \mathrm{BW}/2$, where BW is the beamwidth. The rational for this choice of threshold is that the beam is considered aligned if the AoA/AoD differs from the main beam direction by less than half the beamwidth. This threshold is represented by the dashed lines in Fig. 2. The results are given in Table I. Since both the AoA and AoD are set to be driven by process noise of the same variance, the results for both AoA and AoD are similar. The duration that tracking stays valid increases with the SNR, where the large jump is between 10 dB and 20 dB. This means that tracking does not work well at low SNR and there is a saturation at high SNR. The saturation at high SNR is expected because the driven process noise will still cause the error to accumulate.

B. Effect of Array Size

Fig. 3 shows the MSE plots of the tracking algorithm at SNR of 20 dB for $\sigma_{\mathrm{A}}^2 = \sigma_{\mathrm{D}}^2 = (0.5°)^2$ and $\sigma_{\mathrm{A}}^2 = \sigma_{\mathrm{D}}^2 = (0.25°)^2$

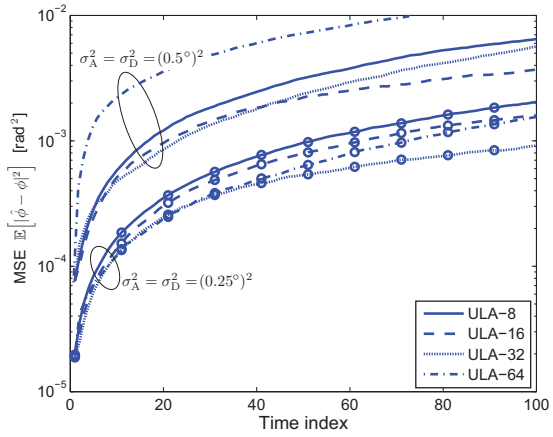

Fig. 3. MSE of the tracking algorithm at SNR of 20 dB for two levels of variation in AoA/AoD ($\sigma_{\rm A}^2$ and $\sigma_{\rm D}^2$) for different array sizes.

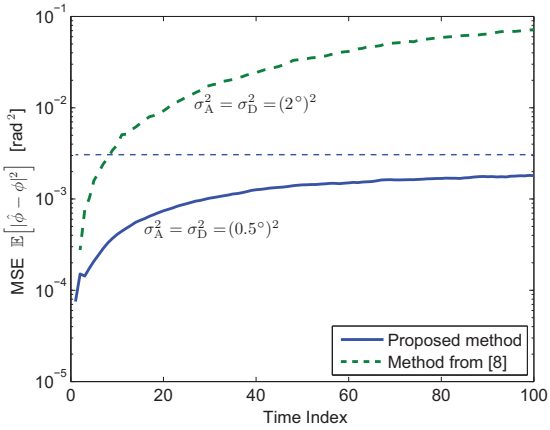

Fig. 4. Comparison of tracking performance of the proposed method with the method in [8]. For fair comparison, we assume slower updating rate (i.e., larger $\sigma_{\rm A}^2$ and $\sigma_{\rm D}^2$) to reflect the higher measurement overhead of the method in [8]. We set $N_{\rm t}=N_{\rm r}=16$ and SNR to 20 dB. α is random but time-invariant.

using different array sizes. Similarly as before, the initial AoA and AoD of 45°, $\rho=0.995$ are used. The SNR definition used here is the SNR including the antenna gains. This ensures that the same measurement noise is experienced by all the array sizes.

From the results in Fig. 3, we observe that the optimal array size depends on the speed of angular changes. At slower angular changes of $(0.25^\circ)^2$, a narrower ULA-32 performs best, while for faster changes of $(0.5^\circ)^2$, a wider ULA-16 performs best. One explanation for this is the characteristics of the measurement function $h(\cdot;\bar{\phi})$ which depend on the array size. Large arrays have narrower beams which is more sensitive to the change in the AoA/AoD so that the tracking accuracy can be expected to be higher. When the beam becomes too narrow as in the ULA-64 for $(0.5^\circ)^2$ in Fig. 3, the performance becomes much worse than other smaller arrays. This is because when the beam becomes too narrow, the process noise could cause the AoA/AoD to be out of the range of being aligned (i.e., larger than half of the beamwidth), which will cause degradation in the observation and will lead to poor tracking capability. Therefore, we conclude from this result that the array size (and thus the beamwidth) has to be chosen appropriately in according with the rate of the change in AoA/AoD for optimal performance. Too small arrays are not sensitive enough to the change in the AoA/AoD, while too large arrays may experience misalignment during the measurement.

C. Comparison to prior work in [8]

Finally, we compare our approach to the prior work in [8]. The method in [8] uses a full scan of all beam combinations as the measurement in each tracking step. For example, for ULA-16 case, this means that this method needs $16\times16=256$ measurements, while our approach requires the measurement of only one beam pair. Generally, the method in [8] requires $N_{\rm t}N_{\rm r}$ times more measurement overhead than our approach. Therefore for a fair comparison, the method in [8] should update at a slower rate (i.e., experiencing higher angular speed changes $\sigma_{\rm A}^2$ and $\sigma_{\rm D}^2$) to offset for the larger overhead.

Fig. 4 shows the result when the angular changes are set to be 16 times faster. Here $N_{\rm t}=N_{\rm r}=16$ and SNR of 20 dB are used. Following [8], α is pecked random at the start of each simulation run but is time-invariant. The method in [8] with 16 times more overhead performs much worst than our approach. If the overhead is set to be equal, the error in the method in [8] becomes too large to be shown in Fig. 4. Therefore, we conclude that due to the faster update rate thanks to the lower measurement overhead, our method is more suitable for beam tracking applications in fast changing environments.

V. Conclusion

MmWave is a promising technology for future wireless networks. A main challenge for mmWave is the need for beamforming. For analog architecture, beamforming can be accomplished by beam training, which requires significant overhead especially in mobile settings. This work proposed a beam tracking algorithm as a solution to reduce the overhead of beam training. The proposed approach only needs the measurement of a single beam pair to track a certain propagation path. Several effects on the performance were investigated. One interesting effect was the array size. At the same SNR, the array should be chosen to be large enough for optimal performance. Arrays that are too small are not sensitive enough to the change in the AoA/AoD, while arrays that are too large could cause misalignment during the measurement.

Acknowledgment

This research is supported in part by the U.S. Department of Transportation through the Data-Supported Transportation Operations and Planning (D-STOP) Tier 1 University Transportation Center and by a gift from TOYOTA Info Technology Center, U.S.A., Inc.

REFERENCES

[1] "IEEE std 802.11ad-2012," *IEEE Standard*, pp. 1–628, Dec. 2012.

[2] WirelessHD, "WirelessHD specification version 1.1 overview," May 2010. [Online]. Available: http://www.wirelesshd.org/

[3] F. Boccardi, R. W. Heath Jr., A. Lozano, T. L. Marzetta, and P. Popovski, "Five disruptive technology directions for 5G," *IEEE Communications Magazine*, vol. 52, no. 2, pp. 74–80, Feb. 2014.

[4] V. Va, T. Shimizu, G. Bansal, and R. W. Heath Jr., "Millimeter wave vehicular communications: A survey," *Foundations and Trends in Networking*, vol. 10, no. 1, 2016.

[5] J. Wang, Z. Lan, C. woo Pyo, T. Baykas, C.-S. Sum, M. Rahman, J. Gao, R. Funada, F. Kojima, H. Harada, and S. Kato, "Beam codebook based beamforming protocol for multi-Gbps millimeter-wave WPAN systems," *IEEE Journal on Selected Areas in Communications*, vol. 27, no. 8, pp. 1390–1399, Oct. 2009.

[6] K. Hosoya, N. Prasad, K. Ramachandran, N. Orihashi, S. Kishimoto, S. Rangarajan, and K. Maruhashi, "Multiple sector ID capture (MIDC): A novel beamforming technique for 60-GHz band multi-Gbps WLAN/PAN systems," *IEEE Transactions on Antennas and Propagation*, vol. 63, no. 1, pp. 81–96, Jan. 2015.

[7] S. Hur, T. Kim, D. J. Love, J. V. Krogmeier, T. A. Thomas, and A. Ghosh, "Millimeter wave beamforming for wireless backhaul and access in small cell networks," *IEEE Transactions on Communications*, vol. 61, no. 10, pp. 4391–4403, Oct. 2013.

[8] C. Zhang, D. Guo, and P. Fan, "Tracking angles of departure and arrival in a mobile millimeter wave channel," in *Proc. of the IEEE International Conference on Communications*, May 2016.

[9] Y. Inoue, Y. Kishiyama, Y. Okumura, J. Kepler, and M. Cudak, "Experimental evaluation of downlink transmission and beam tracking performance for 5G mmW radio access in indoor shielded environment," in *Proc. of the IEEE International Symposium on Personal, Indoor and Mobile Radio Communications*, Aug. 2015, pp. 862–866.

[10] Q. Duan, T. Kim, H. Huang, K. Liu, and G. Wang, "AoD and AoA tracking with directional sounding beam design for millimeter wave MIMO systems," in *Proc. of the IEEE International Symposium on Personal, Indoor and Mobile Radio Communications*, Aug. 2015, pp. 2271–2276.

[11] A. Maltsev *et al.*, "MiWEBA D5.1: Channel modeling and characterization," MiWEBA project, Tech. Rep., Jun. 2014.

[12] R. W. Heath Jr., N. Gonzalez-Prelcic, S. Rangan, W. Roh, and A. Sayeed, "An overview of signal processing techniques for millimeter wave MIMO systems," *IEEE Journal of Selected Topics in Signal Processing*, vol. 10, no. 3, pp. 436–453, Apr. 2016.

[13] C. A. Balanis, *Antenna Theory: Analysis and Design*, 3rd ed. Wiley-Interscience, 2005.

[14] B. Ristic, S. Arulampalm, and N. Gordon, *Beyond the Kalman filter : particle filters for tracking applications*. Artech House Boston, Ma. ; London, 2004.

[15] T. Kailath, A. Sayed, and B. Hassibi, *Linear Estimation*. Pearson, 2000.